Colloid Polym Sci 274:696–702 (1996)

SHORT COMMUNICATION

M. Antonietti
H.-P. Hentze

Synthesis of sponge-like polymer dispersions via polymerization of bicontinuous microemulsions

Received: 18 January 1996
Accepted: 29 January 1996

Dr. M. Antonietti (✉) · H.-P. Hentze
Max-Planck-Institut für Kolloid- und Grenzflächenforschung
Katnstraße 55
14513 Teltow-Seehof, FRG

Abstract Polymer gels with high water content are made by polymerization of hydrophilic/hydrophobic monomer mixtures in bicontinuous microemulsions. These structures can be described as a heterophasic, bicontinuous polymer colloid-in-water structure, the characteristic length of which is only indirectly influenced by the original microemulsion mixture.

The structure formation and phase changes throughout the polymerization reaction are followed with rheology, polarization microscopy, and scanning and transmission electron microscopy. It is shown that already the very first formed polymer changes disturb the bicontinuous phase structure and nucleate a vesicular phase; with further consumption of the monomer mixture, at least three other phase transitions can be detected, ending with a simple globular surfactant structure.

Although direct templating of the original mesomorphous structure does not occur, the existence of the diverse lyotropic phases influences the final structure. It is shown that simple dilution changes the characteristic length of the network elements from about 2 μm down to 50 nm. This is explained by a combination of a nucleation-and-growth mechanism with the influence of a restricted colloidal stability in anisometric lyotropic phases.

Key words Polymerization in bicontinuous microemulsions – interaction of polymers with lyotropic phases – sponge-like polymer dispersions

Introduction

Polymerization in globular microemulsions is a new technique which usually results in ultrafine polymer latices in a size range between 5 nm $< R <$ 50 nm with a narrow particle size distribution (for reviews, see refs. [1, 2]). The polymerization of a hexagonal, lamellar or bicontinuous microemulsion phase preserving the lyotropic order however is still a dream. In most cases, the phase structure is broken up, and simple polymer latices are obtained [3–7]. The formation of dispersed latex particles is prohibited when a water- and an oil-soluble monomer are copolymerized; here, gel-like or sponge-like structures are obtained. Cheung et al. were the first who examined such recipes [8–12]. Their system was composed of methylmethacrylate, ethyleneglycoldimethacrylate (hydrophobic) and acrylic acid (hydrophilic). In no case was the original microemulsion structure maintained, but porous materials with a bicontinuous structure on a length scale of some micrometers were obtained. Ng et al. slightly modified this recipe and copolymerized methylmethacrylate, ethyleneglycoldimethacrylate (oil soluble) and hydroxyethylmethacrylate (water soluble) in the common bicontinuous phase with dodecyltrimethylammoniumbromide as the surfactant [13–15]. With scanning electron microscopy

they showed that the resulting gel-network consists of primary latex particles which coagulate and get cross-linked while the hydrophilic monomer is important to gain interparticular cross-linking. It was also demonstrated that the resulting structures clearly are kinetically frozen-in and do not represent thermodynamic equilibrium states, since marked differences between the structures on top and on the bottom of the reaction ampule were obtained. Depending on the relative water content closed pore structures as well as bicontinuous structures are obtained. The characteristic pore size depends on surfactant concentration and is controlled to be in the range of 0.2–3 μm.

In all cases, the water soluble monomer acts as a cosurfactant for the formulation of the microemulsion, and rather broad bicontinuous phase regions are obtained. Polymerization of the cosurfactant means destabilization of each phase morphology with time, and a decomposition towards microdroplets has to be expected. Preserving an interesting structure at the end of polymerization is winning a race between the cross-linking copolymerization reaction and the decomposition of the microemulsion phase.

In the present paper, we want to illuminate the underlying phase phenomena during this process by following the reaction with polarization microscopy and rheological measurements; these data are compared with the pictures of scanning electron microscopy of the final products. The goal of these trials is a better control about the morphology of the structures also to enable an effective surface functionalization of the structures which is currently excluded.

From a chemical point of view, we chose the copolymerization of styrene and acrylic acid in the common bicontinuous phase with cetyltrimethylammoniumchloride (CTMA) for examination. This special system was chosen due to its simplicity; in addition, the resulting copolymers exhibit amphiphilic properties and might be interesting as polymeric stabilizers of hydrophobic colloids and thickeners by themselves.

Experimental part

Polymerization in bicontinuous phases

Cetyltrimethylammoniumchloride (25% in water) was used as received; the chloride was chosen since it shows a lower tendency towards crystallization and the formation of hexagonal phases. For higher surfactant concentrations, also a freeze-dried powder was prepared. Styrene and acrylic acid are freshly distilled prior to use. All chemicals were supplied by Aldrich Co.

In a typical reaction, 2.00 g CTMA and 6.00 g water are filled in an ampule, and a mixture of 1.00 g acrylic acid, 0.92 g styrene, 0.085 g m-diisopropenylbenzene (cross-linker), and 25 mg AIBN is added. The mixture homogenizes quite rapidly to an optically clear microemulsion, which is equilibrated for another 4 h by stirring at room temperature. The mixture is polymerized by heating the system to 55.0° for 24 h.

Rheological measurements

In order to investigate the process of gelation and the phase behavior, small-amplitude oscillatory shear measurements were taken during the reaction course. For this purpose, a Bohlin CVO-50 rheometer with Cone/Plate Measuring Geometry CP 1/40 was used. We applied a plate radius of 20 mm. The cone angel was 1°. The dynamic storage and loss moduli, G' and G'', were measured at the reaction temperature of 55 °C in a reacting mixture with a constant shear frequency of $\omega = 2$ Hz and a strain of 0.02.

Polarization microscopy

Before and during polymerization the phase behavior of the system was examined by visual observation and polarization microscopy. For scanning the phase diagram samples with different contents of water, surfactant and monomer mixture were prepared, whereas the mixing ratio of the different monomers was kept constant. The birefringence of lyotropic mesophases like liquid hexagonal and lamellar structures was observed by placing the samples on glass supports between crossed polarizers of an Olympus BH-2 microscope.

Transmission and scanning electron microscopy

Transmission electron microscopy (TEM) was used to investigate the formation of the polymer morphology. Most samples were taken during the course of reaction before the gelation occurs. The samples were prepared by dropping the dilute solution onto a copper TEM grid covered with carbon films; after drying, the samples were shadowed with platinum/iridum and carbon. A Tesla BS 500 transmission electron microscope was used for the examination of the contrasted samples. The morphology of the obtained polymer gels was examined using scanning electron microscopy (SEM). The porous polymers were dried by the critical point technique after a gradient exchange of the water against acetone. The dried and freeze

Table 1 List of the samples used in this examination and their chemical compositions. The first two columns give the relative weight content of surfactant and monomers in the reaction mixtures, respectively. m_S/m_M is the weight ratio of surfactant to monomer, m_M/m_W the weight ratio of monomer to water which was kept constant for a set of experiments, each

Sample	% CTMA	% monomer	% H_2O	m_S/m_M	m_M/m_W
M4V2	18.26	20.89	60.85	0.87	0.34
M4V3	15.18	17.37	67.45	0.87	0.26
M4V4	12.99	14.86	72.15	0.87	0.21
M4V5	7.54	8.63	83.82	0.87	0.10
M5V1	12.96	22.25	64.79	0.58	0.34
M5V3	22.94	19.69	57.36	1.17	0.34

fractured samples were sputtered using a palladium target and examined with a Zeiss DSM 940 A or a Tesla BS 340 scanning electron microscope.

Results and discussion

All samples show after polymerization a gel-like appearance and can easily be handled as soft solids in bulk after cracking the ampule. The samples with high water content are translucent and just slightly opaque and exhibit a low modulus, whereas the samples with lower water content are milky white and a have a rather high modulus. Table 1 summarizes the compositions and some of the properties of the set of samples used for the further examination.

For a screening of the significant phase and morphology changes, the reaction was performed in the rheometer. The storage and loss modulus at a fixed frequency (2 Hz) in dependence of the reaction time is shown for two different samples with different water contents in Figs. 1a (M4V4, 72 w% H_2O) & 1b (M4V5, 84 w% H_2O).

Undoubtedly, the observed viscosity increase results from a very complicated overlap of the behavior of the lyotropic structures being present in the systems and the creation of the continuous gel structure. Since we expect for the latter effect the viscosity to increase continuously with time, each stepwise change can be attributed to a change of the lyotropic order.

Although the time scale of the rheology curves differs by a factor of 5, which is related to the influence of the different monomer concentrations on kinetics, we observe in both runs three moduli steps at about the same amount of reaction (note that the scale of the figure is logarithmic, i.e., the steps are well pronounced).

Winter and Chambon had pointed out [16] that a rheological criterion for gelation is $G' \sim G'' \sim \omega^{\alpha}$, with $\tan\delta = \tan(\alpha \cdot \frac{\pi}{2})$. As a first approximation to localize the gel point, we choose $G' = G''$ (a minor mistake is invisible in the logarithmic scale of our experiment), with gels having $G' > G''$. The first step in the moduli curves is towards lower moduli and occurs around the gelation threshold. Also, within the gelled state two additional phase transitions are detected, the first to increase both G' and G'', the second to lower the moduli. Although we cannot relate these transitions to a certain type of morphology transition by rheology, solely, we know them to occur, and we can clearly exclude the presence of a bicontinuous lyotropic structure already at the gel point. In the very early stages of reaction, the viscosity is too low to be accurately measured by the used transducer.

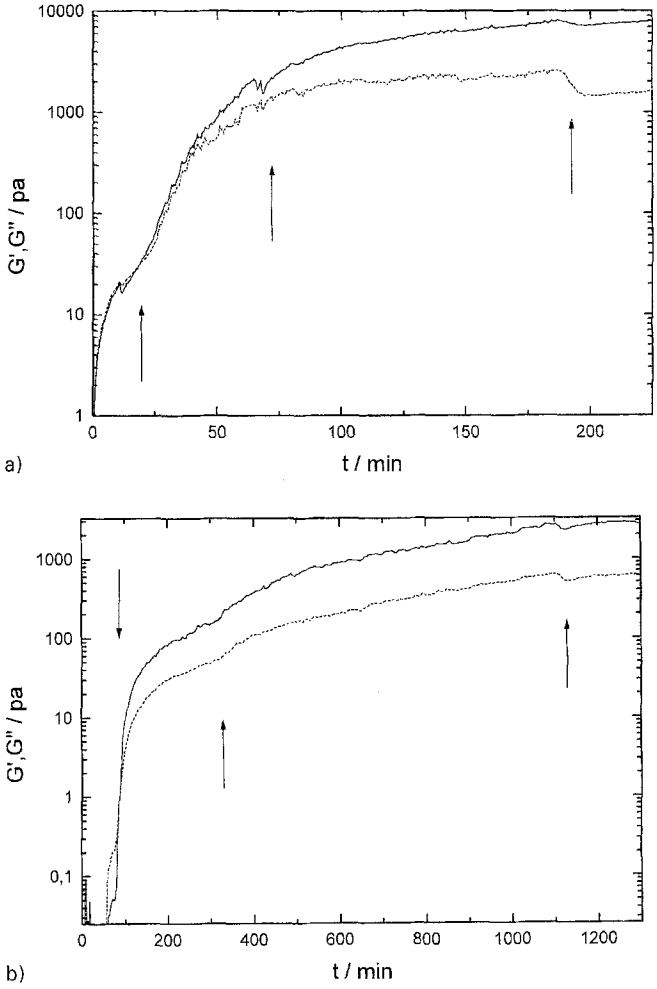

Figs. 1A & B Storage modulus G' (continuous line) and loss modulus G'' (dashed line) versus polymerization time for two different samples: M4V4 (a) and M4V5 (b). Although time scale and moduli are rather different, which is due to a different monomer concentration, both curves show the common features of the reaction kinetics in such systems. No less than three stepwise changes of the moduli are observed (arrows), which are attributed to lyotropic phase changes

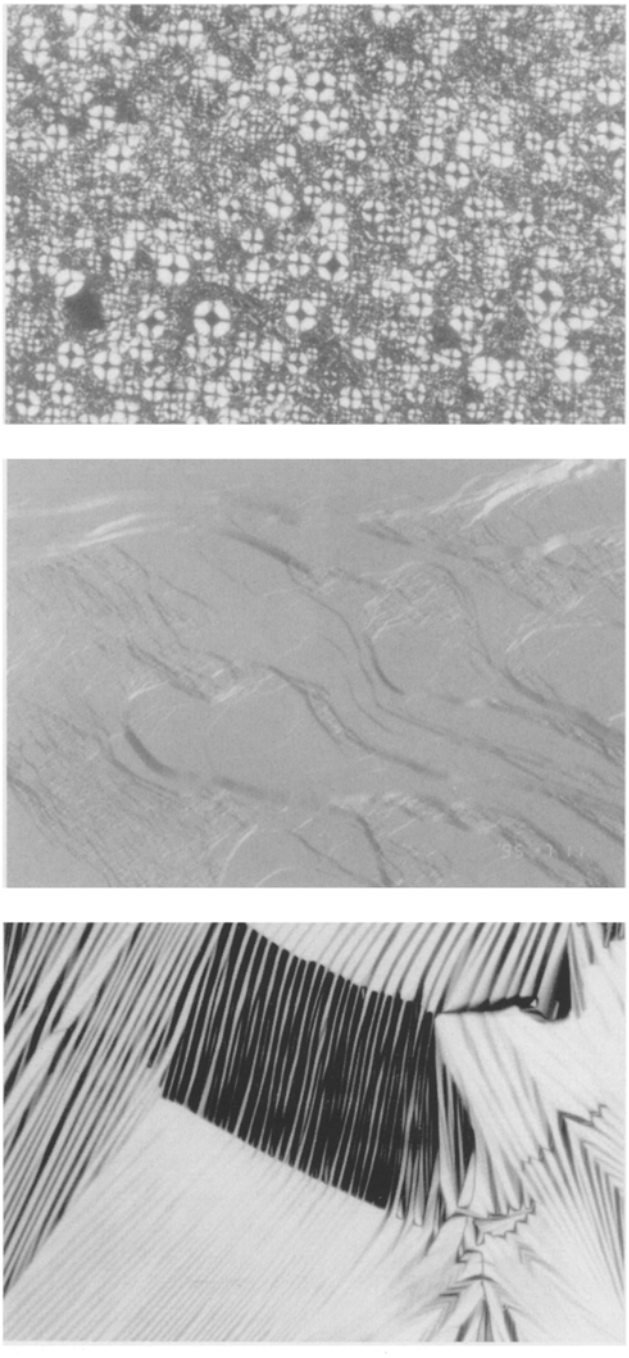

Figs. 2A, B & C Polarization micrographs of the reaction mixtures at different stages of reaction: a) maltese crosses typical for nucleated multilamellar vesicles in the liquid state; b) spider web texture typical for a lamellar mesophase. The spider web texture usually coexists with some maltese crosses. c) fan texture typical for the hexagonal mesophase

In this "liquid" region, observations by the naked eye and polarization microscopy are very helpful. Already well before the first modulus change, the reaction mixture is getting turbid. The onset of turbidity is not accompanied by formation of larger particles which are visible in the microscope; moreover, we observe with polarization microscopy the occurrence of a large number of maltese crosses, as shown in Fig. 2a. This texture is typical for multilamellar vesicles.

The transformation of a bicontinuous microemulsion to a lamellar phase close to an interface is not unusual. Recently, Wennerström et al. published on the behavior of a bicontinuous microemulsion in a force apparatus [17]. They clearly showed that a lamellar phase is induced in direct proximity to the mica surfaces. In our opinion, we can transfer these observations to the here described experiment: nucleating polymer particles modify the bicontinuous structure in such a way that they form the nuclei of multilamellar vesicles. With transmission electron microscopy, we find in this region of reaction separated monodisperse, spherical latex particles with a size in the order of $d = 50$ nm. The small core and an onion-like multilamellar vesicle structure explains that in light microscopy particles are visible in the polarization mode only.

It is already in this very early stage of the reaction where the polymerization of the bicontinuous microemulsion fails. Obviously, the very first polymer chains are not commensurable with the lyotropic order; they homonucleate to latex particles which again change the phase morphology. Since the consumption of cosurfactant at this stage of the reaction is low, we can exclude composition changes to be responsible for the failure. Interestingly, it is the formed polymer particle which destabilizes its own template phase by its different symmetry.

With further progress of reaction, no significant growth of the polymer particles inside their multilamellar corona is observed, it is just that their number is increasing. After that period, the maltese crosses are coexisting with a lamellar phase which become visible also with polarization microscopy. This is shown in Fig. 2b where the spider-web texture typical for lamellar order is shown. It must be underlined that the lamellar phase becomes visible close to the first modulus jump, i.e., it is very probable that the whole reaction mixture is in progress to change from a bicontinuous to a lamellar morphology. A more quantitative statement is hard to make, since the onset of this reaction period heavily depends – as expected – on temperature, water content and composition. In the water-poor parts of the phase diagram, additionally an inverse hexagonal phase is found, the beautiful fan texture of which is shown in Fig. 2c.

In this reaction period, larger cluster-like structures become visible with the microscope. By switching the polarization contrast, it can already be shown that these clusters are (opposite to the surrounding lyotropic phase) not birefringent, i.e., no long-range order has been

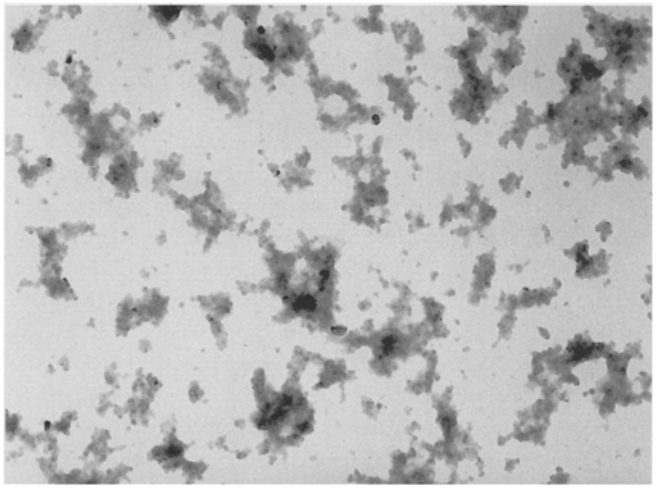

Fig. 3 Transmission electron micrograph of the sample prior to the gel transition (magnification 1:27 000). Scrap-like aggregates of primary spherical particles are observed

imprinted. Again, the local structure of the polymer is not directly influenced by the lyotropic order. However, we cannot exclude an indirect influence on the polymer morphology: in this phase, the primary polymer particles start to coagulate to form the long-range network structure, but not in a random manner. This is probably due to the fact that the two-dimensionally ordered matrix influences the interaction potentials of the colloidal polymer particles in a way that they are forced to coagulate along the lamellae direction while they are stable in direction of the lamellae normal. This phenomenon might also be expressed as some type of depletion demixing of a lyotropic surfactant structure and the spherical polymer particles.

Figure 3 shows a transmission electron micrograph of the clusters slightly before gel transition. One can recognize the small primary latex particles embedded in soft, rather two-dimensional scraps of polymer network.

After gelation, the proceeding of the reaction is hard to follow, since the structure of the soft gel delicately depends on temperature and is influenced by mechanical stress. We can only state that the third step in the viscosity curve is accompanied by a complete loss of briefringence. Since we have consumed most of the cosurfactant at this stage of the reaction, we assume that globular surfactant micelles are formed; the structure is getting isotropic again. Here, the gels also gain their long-term mechanical stability, which is just incompletely described by the moduli at a fixed frequency.

It is interesting to relate these mechanistic findings with the differences observed in the final structures with scanning electron microscopy. Some typical micrographs of structures are shown in Figs. 4a–d, but can be also found in the paper of Ng et al. [15].

In case of high monomer contents, the primary polymer particles grow rather large, whereas for the side of high water contents, a larger number of small particles are formed. This becomes visible from the comparison of Figs. 4b and 4d, which illustrate the width of the accessible size range of the primary particles from about 2 μm down to 50 nm, respectively. This dependence on dilution is in agreement with a homonucleation mechanism with hindered diffusion of the primary polymer chains. It must be underlined that the macroscopic transparency mainly goes with this primary particle size, i.e., the gels consisting of small particles are translucent whereas the others are milky-white.

When the reaction remains rather long in the lamellar period of the reaction (between first and second viscosity jump), also the sponge structure has some tendency to include lamellar structure elements (see Fig. 4c). It was already said that this is certainly not a template effect, since the length scale involved simply exceeds the one of the lyotropic phase by 1–2 orders of magnitude, but might be attributed to a non-isometric colloidal stability inside low-dimensional ordered liquids.

At the end of the reaction, all samples are gel-like samples with a loss angle of $\tan\delta \approx 0.1 - 0.2$ (as already seen in Figs. 1a & b) and absolute values of the storage modulus which agrees well with those of swollen polymer networks with a similar solvent content. This is worth mentioning, since the formed copolymers of styrene and acrylic acid clearly do not dissolve in water and are expected to be in the glassy state. From a technological point of view, it must be underlined that we are able to form a stable water gel on the base of non-dissolved molecules which contains nevertheless up to 84 w% water. This clearly marks the difference to classical polymer dispersions which exhibit a dispersed globular morphology up to polymer contents of 55%.

At the end, we also checked for the influence of the relative surfactant concentration, as expressed in the weight ratio of surfactant to monomer, m_s/m_m (series M5, see Table 1), but keeping the weight ratio of surfactant to water constant. Contrary to the literature [15], we found no pronounced influence of the amount of surfactant on the pore size of the final structure. Within the presented model, this might be expected, since the amount of surfactant only indirectly influences the size of the structures via the appearance of different phase structures at different stages of reaction; there is always a large surplus of surfactant molecules which do not directly interact with the polymer surface, a fact which prevents a more direct influence.

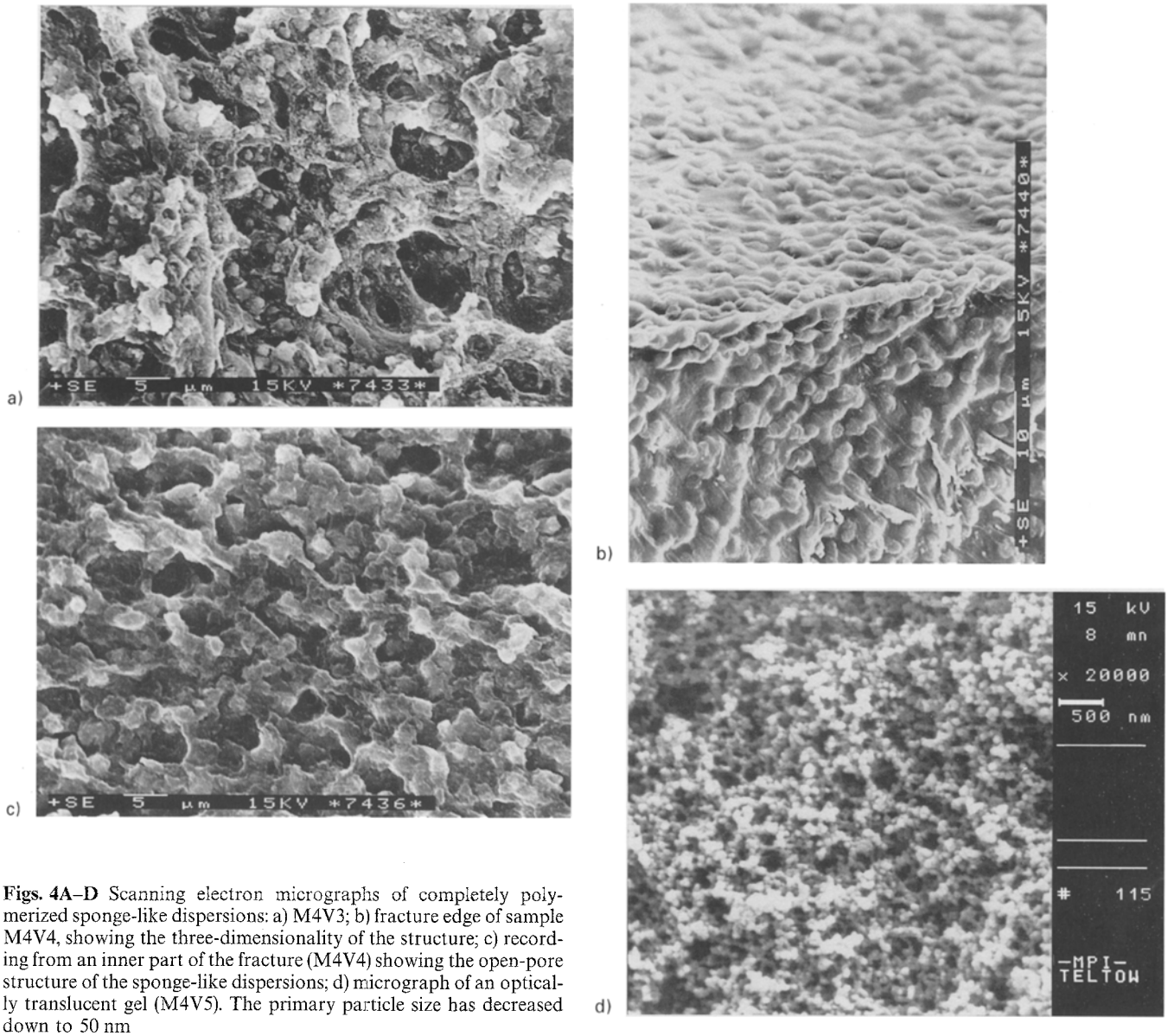

Figs. 4A–D Scanning electron micrographs of completely polymerized sponge-like dispersions: a) M4V3; b) fracture edge of sample M4V4, showing the three-dimensionality of the structure; c) recording from an inner part of the fracture (M4V4) showing the open-pore structure of the sponge-like dispersions; d) micrograph of an optically translucent gel (M4V5). The primary particle size has decreased down to 50 nm

Conclusion and outlook

A combination of a variety of techniques was applied for the examination of the polymerization of hydrophobic/hydrophilic monomer mixtures in bicontinuous microemulsions.

It was shown that templating of the original microemulsion structure does not occur: the polymer chains formed in the very early stages form spherical aggregates, which again nucleate multilamellar vesicles. Further consumption of the monomer mixture leads to the appearance of three other phase transitions, as observed by rheology. With polarization microscopy, indication for a lamellar as well as hexagonal mesophase can be given. These surfactant structures are independent of the colloidal network, since they take place in the water phase, only.

However, it was shown that the final structure is indirectly influenced by the existence of the diverse lyotropic states. The characteristic length of the network elements can be varied between some μm down to 50 nm by the monomer concentration, only. In addition, the connectivity between the element seems to be controlled by the type of lyotropic phase where the cross-linking is performed in. This is speculatively explained by a combination of a nucleation-and-growth mechanism with the

influence of a restricted colloidal stability in anisometric lyotropic phases.

A better handling of this procedure however requires a better understanding of the interaction of colloidal objects with lyotropic phases; such an understanding might also give rise to a controlled "colloidal imprinting" rather than the "molecular imprinting," which was the original goal of these and similar efforts.

The bicontinuous, mechanically stable, open pore structure of the present sponge-like dispersions in combination with their high water content and the mesoporous character in the micrometer range gives rise to a number of interesting potential applications. The development of more effective gel electrophoresis material from non-toxic monomers certainly belongs to some of the more direct uses which has to be explored. In future work, we will also examine some routes towards the functionalization of such materials by incorporation of block copolymers and enzymes into the surface of the mesoporous materials, thus resulting in high-surface sensor coatings or reactive membranes.

Acknowledgments We want to thank Jürgen Hartmann for his enthusiastic help with electron microscopy. Financial support by the Otto-Röhm-Gedächtnisstiftung and the Max Planck Society is gratefully acknowledged.

References

1. Candau F (1992) In: Paleos CM (ed) Polymerization in organized Media. Gordon Science Publ, Philadelphia
2. Antonietti M, Basten R, Lohmann S (1995) Macromol Chem Phys 196:441
3. Candau F, Zekhnini Z, Durand JP (1986) J Coll Interfac Sci 114:398
4. Holtzscherer C, Candau F (1988) Colloid Surf 29:411
5. Holtzscherer C, Candau F (1988) J Colloid Interface Sci 125:97
6. Candau F (1989) In: El-Nokaly M (ed) Polymer Assosciation Structures: Microemulsions and Liquid Crystals, ACS Symp Series 384:48
7. Holtzscherer C, Wittmann JC, Guillon D, Candau F (1990) Polymer 31:1978
8. Palani Raj WR, Sasthav M, Cheung HM (1991) Langmuir 7:2586
9. Palani Raj WR, Sasthav M, Cheung HM (1992) J Colloid Interfac Sci 152:376
10. Palani Raj WR, Sasthav M, Cheung HM (1992) Langmuir 8:1931
11. Palani Raj WR, Sasthav M, Cheung HM (1993) J Appl Polym Sci 47:599
12. Palani Raj WR, Sasthav M, Cheung HM (1993) Polymer 34:3305
13. Gan LM, Chieng TH, Chew CH, Ng SC (1994) Langmuir 10:4022
14. Chieng TH, Gan LM, Chew CH, Ng SC (1995) Polymer 36:1941
15. Chieng TH, Gan LM, Chew CH, Lee L, Ng SC, Pey KL, Grant D (1995) Langmuir 11:3321
16. Chambon F, Winter HH (1986) J Rheol 30/2:367
17. Petrov P, Miklavcic S, Olsson U, Wennerström H (1995) Langmuir 11:3928